Communication

Enhanced Activity for Oxygen Reduction Reaction on "PtCo" Nanoparticles: Direct Evidence of Percolated and Sandwich-Segregation Structures

Shuo Chen, Paulo J. Ferreira, Wenchao Sheng, Naoaki Yabuuchi, Lawrence F. Allard, and Yang Shao-Horn
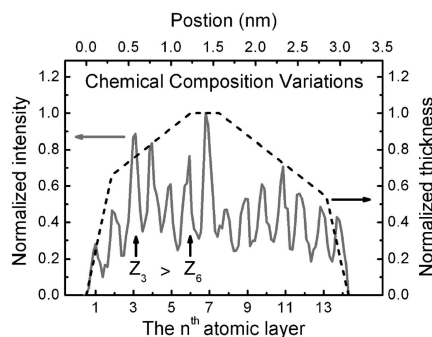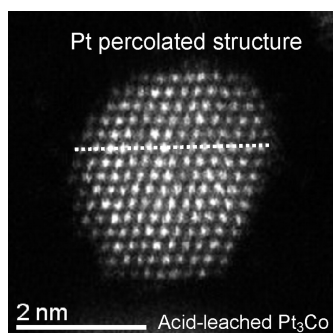
More About This Article

Additional resources and features associated with this article are available within the HTML version:

- Supporting Information
- Access to high resolution figures
- Links to articles and content related to this article
- Copyright permission to reproduce figures and/or text from this article

View the Full Text HTML

Enhanced Activity for Oxygen Reduction Reaction on "Pt₃Co" Nanoparticles: Direct Evidence of Percolated and Sandwich-Segregation Structures

Shuo Chen,[†] Paulo J. Ferreira,[‡] Wenchao Sheng,[†] Naoaki Yabuuchi,[†] Lawrence F. Allard,[§] and Yang Shao-Horn*,[†]

Electrochemical Energy Laboratory, Massachusetts Institute of Technology, Cambridge, Massachusetts 02139, Materials Science and Engineering Program, The University of Texas at Austin, Austin, Texas 78712, and Oak Ridge National Laboratory, Oak Ridge, Tennessee 37831

Received April 6, 2008; E-mail: shaohorn@mit.edu

Oxygen reduction reaction (ORR) limits the efficiency of fuel cells, and thus it is of great interest to discover nanocatalysts with an ORR activity superior to that of Pt.[1] Recent research efforts have been focused on understanding surface chemistry and electronic structures on Pt alloy model surfaces that exhibit an ORR activity higher than that of Pt.[2] On bulk Pt alloy surfaces, Pt can segregate in the outermost layer to form a "sandwich-segregation"[3] or "Pt-skin structure",[2e] which is shown to weaken the metal−oxygen bond strength relative to Pt[4] and increase specific ORR activity (based on Pt surface area). In addition, pure Pt on the outermost surface layer can be obtained on Pt alloys by acid removal of transition metals,[2d,e,5] and such surfaces also exhibit enhanced ORR activity relative to Pt. It is essential to examine if the ORR mechanisms established for bulk Pt alloy surfaces are applicable to tailoring the activity of Pt alloy nanoparticles. Pt alloy nanoparticles[6] are known to exhibit specific ORR activity 2−5 times higher than that of Pt. However, the origin in the enhancement of ORR activity of Pt alloy nanoparticles is not understood, as little is known about chemical compositions of near-surface regions of nanoparticles.

In this work, we show chemical compositions of "Pt₃Co" nanoparticles at the atomic scale using aberration-corrected scanning transmission electron microscopy (STEM), from which the origin of ORR activity enhancement of Pt alloy nanoparticles is postulated. Chemical composition variations within individual nanoparticles of acid-treated "Pt₃Co" were observed, which is in good agreement with the formation of percolated Pt-rich regions that extend from the surface to the particle center (analogous to the skeleton structure proposed previously for bulk Pt alloy surfaces[2d,e] after acid leaching). Upon annealing of such acid-treated nanoparticles, direct evidence of Pt sandwich-segregation surfaces[3] of ordered "Pt₃Co" nanoparticles was found. The enhanced ORR activity (normalized to Pt surface area) of acid-treated and annealed "Pt₃Co" nanoparticles relative to Pt nanoparticles was attributed to compressive strains and ligand effects associated with the percolated and sandwich-segregation structures in nanoparticle near-surface regions, respectively.

Acid-treated "Pt₃Co" supported on carbon (46 wt% Pt) with an average atomic Pt/Co ratio of 3.6 (having a number-averaged particle size of ∼4 nm) was prepared from leaching of a "PtCo" sample in acid by Tanaka Kikinzoku Kogyo (TKK). Acid-treated nanoparticles were subsequently heat-treated at 1000 K for 3 h in a vacuum (∼10⁻² Torr). Annealed "Pt₃Co" was found to have a number-averaged particle diameter of ∼5 nm. A sample of Pt nanoparticles supported on carbon (having a number-averaged

† Massachusetts Institute of Technology.
‡ The University of Texas at Austin.
§ Oak Ridge National Laboratory.
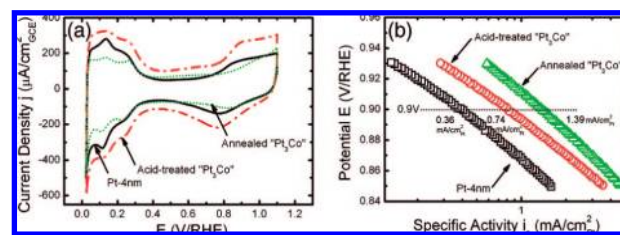
Figure 1. (a) Cyclic voltammograms of Pt-4nm, acid-treated, and annealed "Pt₃Co" collected in N₂-saturated 0.1 M HClO₄ (room temperature and 50 mV/s). (b) Tafel plots obtained from polarization curves collected in O₂-saturated 0.1 M HClO₄ on a rotating disk electrode in the positive-going scan at 1600 rpm at a sweep rate of 10 mV/s.

diameter of ∼4 nm) was used for comparison, which was prepared from heating supported Pt nanoparticles diameter (∼2 nm, TKK, 46 wt% Pt) to 1173 K in Ar. Particle size histograms and average diameters of these samples are shown in Supporting Information Figure S1a−c and Table S1.

The ORR activity of "Pt₃Co" and Pt nanoparticles was measured by sweep voltammetry in O₂ saturated HClO₄ electrolyte using a rotating disk electrode at room temperature (Figure S2). Cyclic voltammetry of "Pt₃Co" nanoparticles was performed in O₂ free electrolyte (Figure 1a), from which the electrochemical active area was obtained from integrating the charge associated with hydrogen desorption. The specific ORR activity of acid-treated and annealed "Pt₃Co" nanoparticles normalized to the Pt surface area was compared with that of Pt nanoparticles as a function of potential in Figure 1b and Table S1. At 0.9 V vs RHE, the activity of acid-treated "Pt₃Co" nanoparticles is ∼0.74 mA/cm²$_{Pt}$ (∼2 times that of Pt), which is comparable to acid-leached Pt alloy nanoparticles reported previously.[1] On the other hand, the specific activity of annealed "Pt₃Co" at 0.9 V vs RHE was increased to ∼1.39 mA/cm²$_{Pt}$ (∼4 times that of Pt) after annealing.

Aberration-corrected high-angle annular dark-field (HAADF) images recorded using a JEOL 2200FS-AC STEM provided, for the first time, direct evidence of chemical composition variations within individual "Pt₃Co" nanoparticles at the atomic scale. HAADF images (Figure 2a) revealed individual columns of atoms and intensity variations across different columns within each particle. Most acid-leached "Pt₃Co" nanoparticles were found disordered from fast Fourier transforms of HAADF images (Figure S3). The HAADF intensity for each column of atoms is proportional to the product of the square of the average atomic number (Z^2) for each column of atoms and particle thickness. As shown in Figure 2b, nanoparticle thickness changes (dash line) obtained from a truncated octahedron[7] cannot fully account for intensity variations (solid line) observed (Figure S3). It is evident that some columns of atoms
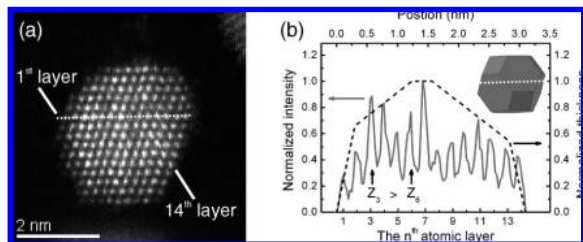
Figure 2. (a) An aberration-corrected HAADF image of an acid-treated "Pt$_3$Co" nanoparticle. (b) Normalized image intensity of the particle in (a) along the dotted line (solid curve), where the average atomic number of the 3rd and 6th column of atoms projected in the beam direction is marked. Dash curve: normalized thickness changes were obtained by assuming a shape of ideal truncated octahedron shown in (b) insert.
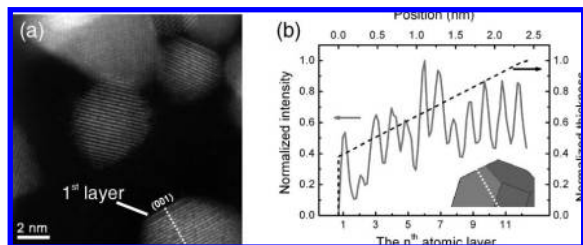
Figure 3. (a) An aberration-corrected HAADF image of annealed "Pt$_3$Co" nanoparticles. Pt segregation in the (100) particle surface was observed on ordered "Pt$_3$Co" ($Pm\bar{3}m$). The bright atomic layer on the surface is Pt-rich while the dark layer(s) is Co-rich. (b) Solid curve: normalized intensity of the particle at bottom (a) along the dotted line; dash curve: normalized thickness variations were obtained by assuming an ideal truncated octahedron particle shape shown in (b) insert.

close to the particle center have lower average atomic numbers than surface regions, which suggests the formation of percolated Pt-rich surface and Pt-poor core regions in acid-treated "Pt$_3$Co" nanoparticles. This proposed structure is different from the core−shell morphology (where pure Pt or Pt enrichment is confined typically near the particle surface regions) reported previously.[6b,d] The proposed percolated structure is further supported by observed HAADF intensity variations within acid-treated "Pt$_3$Co" nanoparticles of ~10 nm (Figure S4), and STEM energy dispersive spectroscopy revealed variation in the Pt/Co atomic ratio across particles (Figure S5). Although further analysis is needed to determine strain distributions with individual particles from STEM HAADF images, it is postulated that the interfacial regions (without or with vacancies[8]) between Pt-rich and Pt-poor regions can result in a shortened Pt−Pt bond distance relative to Pt nanoparticles. The compressed Pt−Pt bond length has shown to lower the valence band center relative to the Fermi level,[4b,9] reduce the binding strength and/or coverage of oxygenated adsorbates,[10] and enhance ORR activity. Surface facets of "Pt$_3$Co" and Pt nanoparticles were examined by high-resolution transmission electron microscopy, and the area fractions of low-index and high-index surfaces were found to be comparable (Figure S6). Therefore, it is proposed that the enhanced activity of acid-treated "Pt$_3$Co" is attributed to compressive strains and ligand effects of the nanoparticle percolated structure.

Comparison between the normalized intensity of aberration-corrected HAADF images (Figure 3a) and normalized particle thickness (Figure 3b) of an annealed "Pt$_3$Co" nanoparticle clearly revealed Pt enrichment in the outermost layer (bright lines) followed by Co enrichment in the second layer (dark line). Pt segregation, typically in the first 1−3 atomic layers on the (100) surface, was found only for ordered "Pt$_3$Co" nanoparticles with the space group $Pm\bar{3}m$ which was confirmed by analyzing fast Fourier transforms of HAADF images (Figure S7). Although Pt segregation has been predicted on truncated-octahedral, disordered Pt$_3$Co nanoparticles,[2d,7] to the authors' knowledge, this is the first time that direct evidence of Pt sandwich-segregation[3a] is shown on the surface of Pt alloy nanoparticles. The enhanced ORR activity (~4 times that of Pt) can be attributed to the Pt sandwich-segregation structure on annealed "Pt$_3$Co" nanoparticles. Not only can Co-rich layers beneath the Pt segregated surface layer(s) compress the surface Pt−Pt bond distance, but also they can induce the ligand effect due to Pt−Co bonds. Combined effects lead to reduced reactivity of surface Pt atoms toward oxygenated adsorbates[2c,d,9c] and increased ORR activity. Therefore, controlling the surface chemical compositions of nanoparticle facets such as inducing Pt segregation by annealing and monolayer synthesis[2a,b] represents a promising route to develop highly active catalysts for ORR in low-temperature fuel cells.

Supporting Information Available: Size distributions, construction of 3D nanoparticles, images of nanoparticle surface atomic structures, and details of electrochemical measurements. This material is available free of charge via the Internet at http://pubs.acs.org.

References

(1) Gasteiger, H. A.; Kocha, S. S.; Sompalli, B.; Wagner, F. T. *Appl. Catal., B* **2005**, *56*, 9–35.
(2) (a) Zhang, J. L.; VukmirovicM. B.; Xu, Y.; Mavrikakis, M.; Adzic, R. R. *Angew. Chem., Int. Ed.* **2005**, *44*, 2132–2135. (b) Nilekar, A.; Xu, Y.; Zhang, J.; Vukmirovic, M.; Sasaki, K.; Adzic, R.; Mavrikakis, M. *Top. Catal.* **2007**, *46*, 276–284. (c) Stamenkovic, V. R.; Fowler, B.; Mun, B. S.; Wang, G. F.; Ross, P. N.; Lucas, C. A.; Markovic, N. M. *Science* **2007**, *315*, 493–497. (d) Stamenkovic, V. R.; Mun, B. S.; Arenz, M.; Mayrhofer, K. J. J.; Lucas, C. A.; Wang, G. F.; Ross, P. N.; Markovic, N. M. *Nat. Mater.* **2007**, *6*, 241–247. (e) Stamenkovic, V. R.; Mun, B. S.; Mayrhofer, K. J. J.; Ross, P. N.; Markovic, N. M. *J. Am. Chem. Soc.* **2006**, *128*, 8813–8819.
(3) (a) Gauthier, Y. *Surf. Rev. Lett.* **1996**, *3*, 1663–1689. (b) Ruban, A. V.; Skriver, H. L.; Norskov, J. K. *Phys. Rev. B* **1999**, *59*, 15990–16000.
(4) (a) Norskov, J. K.; Rossmeisl, J.; Logadottir, A.; Lindqvist, L.; Kitchin, J. R.; Bligaard, T.; Jonsson, H. *J. Phys. Chem. B* **2004**, *108*, 17886–17892. (b) Xu, Y.; Ruban, A. V.; Mavrikakis, M. *J. Am. Chem. Soc.* **2004**, *126*, 4717–4725. (c) Stamenkovic, V.; Mun, B. S.; Mayrhofer, K. J. J.; Ross, P. N.; Markovic, N. M.; Rossmeisl, J.; Greeley, J.; Norskov, J. K. *Angew. Chem., Int. Ed.* **2006**, *45*, 2897–2901.
(5) Toda, T.; Igarashi, H.; Uchida, H.; Watanabe, M. *J. Electrochem. Soc.* **1999**, *146*, 3750–3756.
(6) (a) Mukerjee, S.; Srinivasan, S. *J. Electroanal. Chem.* **1993**, *357*, 201–224. (b) Watanabe, M.; Tsurumi, K.; Mizukami, T.; Nakamura, T.; Stonehart, P. *J. Electrochem. Soc.* **1994**, *141*, 2659–2668. (c) Stamenkovic, V.; Schmidt, T. J.; Ross, P. N.; Markovic, N. M. *J. Electroanal. Chem.* **2003**, *554*, 191–199. (d) Koh, S.; Strasser, P. *J. Am. Chem. Soc.* **2007**, *129*, 12624–12625. (e) Koh, S.; Leisch, J.; Toney, M. F.; Strasser, P. *J. Phys. Chem. C* **2007**, *111*, 3744–3752.
(7) Wang, G.; Van Hove, M. A.; Ross, P. N.; Baskes, M. I. *J. Chem. Phys.* **2005**, *122*, 024706.
(8) Erlebacher, J; Aziz, M. J.; Karma, A.; Dimitrov, N.; Sieradzki, K. *Nature* **2001**, *410*, 450–453.
(9) (a) Mavrikakis, M.; Hammer, B.; Norskov, J. K. *Phys. Rev. Lett.* **1998**, *81*, 2819–2822. (b) Grabow, L.; Xu, Y.; Mavrikakis, M. *Phys. Chem. Chem. Phys.* **2006**, *8*, 3369–3374. (c) Kitchin, J. R.; Norskov, J. K.; Barteau, M. A.; Chen, J. G. *Phys. Rev. Lett.* **2004**, *93*, 156801.
(10) (a) Mukerjee, S.; Srinivasan, S.; Soriaga, M. P.; Mcbreen, J. *J. Electrochem. Soc.* **1995**, *142*, 1409–1422. (b) Mukerjee, S.; Srinivasan, S.; Soriaga, M. P.; Mcbreen, J. *J. Phys. Chem.* **1995**, *99*, 4577–4589. (c) Wakisaka, M.; Suzuki, H.; Mitsui, S.; Uchida, H.; Watanabe, M. *J. Phys. Chem. C* **2008**, *112*, 2750–2755.

JA802513Y